Research in Astronomy and Astrophysics, 23:095023 (13pp), 2023 September https://doi.org/10.1088/1674-4527/ace518

An Overview of FAST Real-time Fast Radio Burst Searching System

X. X. Zhang[1,2], R. Duan[1], V. Gajjar[3], H. Y. Zhang[1,4], P. Wang[1], C. H. Niu[1], D. Werthimer[3,5], J. Cobb[3,5], S. Y. Li[6], X. Pei[7], Y. Zhu[1], and D. Li[1,2,8]

[1] National Astronomical Observatories, Chinese Academy of Sciences, Beijing 100101, China; zhangxinxin@nao.cas.cn, duanran@nao.cas.cn, hyzhang@bao.ac.cn
[2] University of Chinese Academy of Sciences, Beijing 100049, China
[3] Department of Astronomy, University of California Berkeley, Berkeley, CA 94720, USA
[4] Hebei Key Laboratory of Radio Astronomy Technology, Shijiazhuang 050081, China
[5] Space Sciences Laboratory, University of California Berkeley, Berkeley, CA 94720, USA
[6] Beijing Planetarium, Beijing Academy of Science and Technology, Beijing 100044, China
[7] Xinjiang Astronomical Observatory, Chinese Academy of Sciences, Urumqi 830011, China
[8] NAOC-UKZN Computational Astrophysics Centre, University of KwaZulu-Natal, Durban 4000, South Africa
Received 2023 March 24; revised 2023 May 26; accepted 2023 June 15; published 2023 August 21

Abstract

In this paper, we report a real-time Fast Radio Burst (FRB) searching system that has been successfully implemented with the 19 beam receiver of the Five-hundred-meter Aperture Spherical radio Telescope (FAST). The relatively small field of view of FAST makes the search for new FRBs challenging, but its high sensitivity significantly improves the accuracy of FRB localization and enables the detection of high-precision neutral hydrogen absorption lines generated by FRBs. Our goal is to develop an FRB searching system capable of real-time detection of FRBs that allows high-time resolution spectro-temporal studies among the repeated bursts, as well as detailed investigations of these bursts and exploration of FRB progenitor models. The data from each beam of the 19-beam receiver are fed into a high-performance computing node server, which performs real-time searches for pulses with a wide dispersion measure (DM) range of 20–10,000 pc cm^{-3} with step efficiency of 25% in real time. Then, the head node server aggregates all the candidate signals from each beam within a given time, determining their authenticity based on various criteria, including arrival time, pulse width, signal-to-noise ratio and coincidence patterns among the 19 beams. Within the 1.05–1.45 GHz operating bandwidth of the FAST 19 beam receiver, the system achieves a frequency resolution of 122.07 kHz and a time resolution of 270.336 μs. Subsequently, our team detected a series of bursts with a DM of 566 on 2019 August 30 confirming them as FRB 121102. The FRB searching system enables the 19-beam receiver of FAST to detect repeated/one-off pulses/bursts in real time.

Key words: Astronomical Instrumentation – Methods and Techniques – instrumentation: spectrographs – methods: miscellaneous

1. Introduction

Since the discovery of the first Fast Radio Burst (FRB) in 2007 (Lorimer et al. 2007), its study has quickly become one of the frontiers and hotspots of radio astronomy. The precisely localized source FRB 121102 has been dubbed “the most exciting discovery in the field of astronomy since Laser Interferometer Gravitational-Wave Observatory (LIGO) detection” by the American Astronomical Society (Chatterjee et al. 2017). FRBs are currently the brightest bursts in the radio band known in the Universe. Each day, thousands to tens of thousands of burst pulses reach the Earth, and our knowledge of their origin and physical mechanism is far from conclusive. Major international radio telescopes such as Canadian Hydrogen Intensity Mapping Experiment (CHIME) have spent considerable time developing specialized equipment and have produced numerous results in the field of FRB research (Amiri et al. 2019). According to Fast Radio Burst CATalog (FRBCAT) statistics, nearly 1000 FRBs have been discovered, with dozens of them being identified as repeated bursts of FRBs. The critical aspect of this field is to authenticate its counterpart, determine its extragalactic origin hypothesis and comprehend its physical mechanism. This entails optimizing the quality of the discovery while increasing the number, specifically optimizing the positioning accuracy and recording the data generated when the pulse bursts.

Due to Five-hundred-meter Aperture Spherical radio Telescope (FAST)’s relatively small field of view, it does not yield as many new FRBs as large field telescopes such as CHIME. However it has an extremely high sensitivity and the required operating conditions, which are necessary to significantly improve the accuracy of FRB positioning and to detect the high-precision neutral hydrogen absorption line generated by FRBs in real time. As various telescopes expand their FRB observations and the number of discoveries increases significantly, the demand for high-quality discovery becomes more pressing. FAST possesses unique advantages and the potential to make significant contributions to this field.

To begin with, hundreds of discoveries of FRBs have been reported thus far. However as research advances and the number of discoveries continues to grow, the high positioning accuracy provided by the high-sensitivity telescope and the high-precision data generated by the explosion have become critical and indispensable. An FRB is a cosmological target; hence, the absorption line in its signals can be used to determine the true distance of the FRB, the intragalactic medium of the FRB host galaxy and the intergalactic medium at cosmological distances. These will eventually shed light on the true physical nature of FRBs as cosmological phenomena (Li et al. 2018), and pave the way for new and far-reaching scientific breakthroughs. Moreover, thousands to tens of thousands of burst pulses arrive on the Earth each day, and the number of FRBs detected and captured by FAST is significant. FAST has an extremely high sensitivity. When the quantity and quality of FAST discoveries are carefully considered, FAST offers unique advantages and opportunities for significant discoveries in this field. Based on incomplete statistics, there are dozens of models for the origin of FRBs. The current observational limit is woefully inadequate. By implementing the FAST real-time FRB searching system, the observation capabilities for key counterpart certification in this field will be significantly improved.

Moreover, FAST is an ideal instrument to discover repeated bursts from one-off FRBs, with the capability to obtain the world's best signal-to-noise ratio (S/N) and burst rate statistics. In studying the origins of FRBs, researchers found the first repeated source, FRB 121102, exhibited nearly completely linear polarization and a very high Faraday Rotation Measure (RM) (Gajjar et al. 2018; Michilli et al. 2018). The question of whether all repeated burst sources have such a high RM will determine if these bursts are generated by young magnetars or by other mechanisms, such as "combing" the magnetic field of the foreground neutron star by the outflow of a massive black hole (Zhang 2018a). FAST has made significant strides in the investigation of repeated bursts. We achieved the first real-time detection of FRB 121102's repeated bursts in 2019, with the highest burst rate statistics and S/N (Li et al. 2021).

Finally, FAST has the potential to detect the Universe's most distant FRBs. The largest dispersion measure (DM) discovered thus far is 2596.1 (Bhandari et al. 2017), which has a redshift of about 3. FAST can detect FRBs with a redshift greater than 10 based on extrapolation of known FRB data (Zhang 2018b). The discovery of these high redshift FRBs, particularly the discovery of cases with $z > 6$, will significantly advance our understanding of the Universe's evolution, particularly the early ionization process.

Along with the total FRB population increases, and the high time resolution data, sustained monitoring has given us insight into progenitor models (James et al. 2022), however the total number of FRBs found so far is insufficient to distinguish between these models. FAST's 19 beam digital backend has the ability to record high-time resolution data up to 49.152 μs while searching for FRBs in real time, thus enabling spectro-temporal studies among the repeated bursts which also allow FRB progenitor models to be scrutinized.

In this paper we provide a systematic overview of the FAST real-time FRB searching system, including its data processing pipeline and its observation results of the FRB 121102. Section 2 describes the science drivers and unique advantage of FAST FRB detection. Section 3 provides the key parameters for the FAST real-time FRB searching system and its system architecture in detail. A complete explanation of its data processing pipeline is provided in Section 4. Information on the following commission test, CRAFTS observation and candidate confirmation is provided in Sections 5 and 6. In order to improve the flexibility and quality of daily observations, a discussion of future system upgrades is given in Section 7.

2. FAST Real-time FRB Searching System

2.1. Key Parameters of the System

FAST was completed in 2016 and it detected its first spectral line by using an ultra-wideband receiver with a working frequency range of 270–1620 MHz. This receiver is one of seven FAST receivers which completely cover the telescope's operating frequency range of 70 MHz–3 GHz. We developed the China Reconfigurable ANalog-digital backEnd (CRANE) for this ultra-wideband feed and successfully detected the neutral hydrogen absorption line of 3C 409 in drifting scan mode on 2017 August 14 (Zhang et al. 2019). Then the spectra of W49 OH masers at 1612, 1665 and 1667 MHz were detected, and we found their circular polarization is basically consistent with the result of the Arecibo radio telescope. Additionally, to maximize the efficiency of FAST observations, the engineers installed and commissioned the 19-element multi-beam feed. Similarly, this receiver is one of seven FAST receivers, and it was used since the first half of 2018. This receiver generates 19 dual-polarized beams over the frequency range of 1050–1450 MHz, and the receiver system's actual working noise temperature is approximately 24 K (Jiang et al. 2019). No FRB related equipment was planned when the FAST project was established, but as the telescope started commissioning, our team began to develop the FAST real-time FRB searching system, which was designed in parallel with a commensal Search for ExtraTerrestrial Intelligence (SETI) backend. The critical parameters for this system are listed in Table 1.

Table 1
Key Parameters for FAST Real-time FRB Searching System

Parameter	Value
Location	East: 107° 21′, North: 25° 48′
Frequency range (MHz)	1050–1450
Polarization	Orthogonal
Focal ratio	0.467
System temperature (K)	24
decl. range	−14.4°–65.6°
Number of beams	19
Half power beamwidth (@1.4 GHz)	0.052
FRB search time resolution (μs)	270.336
FRB search frequency resolution (KHz)	122.07

2.2. System Structure

The FAST real-time FRB searching system is composed of ten Reconfigurable Open-Architecture Compute Hardware version 2 (ROACH2) designed by the Collaboration for Astronomy Signal Processing and Electronics Research (CASPER), one High-Performance Computing (HPC) head node and nineteen HPC compute nodes equipped with Graphics Processing Units (GPUs), all connected via high-speed Ethernet switches. Table 2 lists the configuration of these compute nodes.

The electromagnetic signal received by the multi-beam feed is collected by a 300 m instantaneous parabolic reflector, then passed through a refrigerated low noise amplifier, ortho-mode transducers and an electro-optic conversion module before being transmitted to the main control room via optical fiber. The onboard Analog to Digital Converters (ADCs) digitize the coaxial cable's radio frequency analog signals. This ADC card is based on a Texas Instruments ADC08D1520[9] low-power ADC chip. The sampling rate of each channel is up to 1.5 Gsps when operating in two-channel mode, and we use a sampling frequency of 1 GHz to sample signals from 1 to 1.5 GHz, fully meeting the bandwidth requirement of the 19 beam receivers. Additionally, each ADC card digitizes two polarization signals from one of nineteen beams. The block diagram of the FAST real-time FRB searching system is drawn in Figure 1. Following the electro-optic modulator, we added a Mini-Circuits bandpass filter ZAFBP-1250-1+ operating at 1050–1450 MHz to filter out stray waves in each polarization signal. Since the multi-beam receiver's digital backend also includes spectral line and pulsar modes, the broadband mode's operating bandwidth is 500 MHz, and all of these backends share the clock signal synthesized by the MODEL SSG-6400HS[10] synthesizer. This USB-based synthesized signal generator will generate a 1 GHz clock signal, which is distributed as the clock input to all the ADCs in the backend of

[9] https://www.ti.com/product/ADC08D1520
[10] https://www.minicircuits.com/pdfs/SSG-6400HS.pdf

Table 2
Compute Node Configuration for FAST Real-time FRB Searching System

Feature	PowerEdge R730 Server
Form factor	2U rack
CPU	Intel Xeon E5-2660 v4
GPU	NVIDIA GTX 1080Ti
NIC	Intel X710
Memory	8*8GB DDR4
Hard drive	8*8TB Dell 7.2K RPM NLSAS

the multi-beam receiver via the power splitter. Figure 2 displays the ROACH boards and servers for the FAST real-time FRB searching system in the Computer Room at the FAST site.

2.3. Synchronization and Clock Synthesizer

The time and frequency standards used in the radio astronomy data recording system are crucial. If the digital backend does not have reliable time accuracy and stable frequency resources, the data recorded by the digital receiver will be unavailable for subsequent data processing. A block diagram of the pulse per second (PPS) and clock is illustrated in Figure 3. The standard time signals are derived initially from Global Positioning System (GPS) time servers with a standard deviation of less than 15 ns in the direction of Coordinated Universal Time (UTC). The system's time precision and stability are approximately 5 ns, which are enhanced by the UTC-NIM Disciplined Oscillator (NIMDO) system. The PPS enables boards to capture data on the PPS's rising edge, synchronizing the boards to within one clock cycle (5 ns) (Zhu et al. 2020).

3. The FAST Real-time FRB Searching System Pipeline

The FAST real-time FRB searching system is primarily responsible for radio astronomy data acquisition, digital signal analysis and processing tasks associated with searching for real-time FRBs via the FAST multi-beam receiver. This backend's firmware is multipurpose. The ROACH2 board generates spectral data streams to support HI/pulsar and FRB searches. Additionally, it can also provide raw data for SETI (Zhang et al. 2020) or baseband data analysis. The data packets contain well-designed IP and MAC addresses for their destinations. Through the multi-cast mechanism, the high-speed Ethernet switches can duplicate and spread the packets to different Network Interface Cards (NICs). Thus, the 19 beam digital backend can simultaneously receive the pulsar or spectral line data for offline search while searching for FRBs and searching for SETI signals. The onboard FPGA, which is firmware-programmed, then performs 4096 points of FFT channelization on these digital signals and packages the

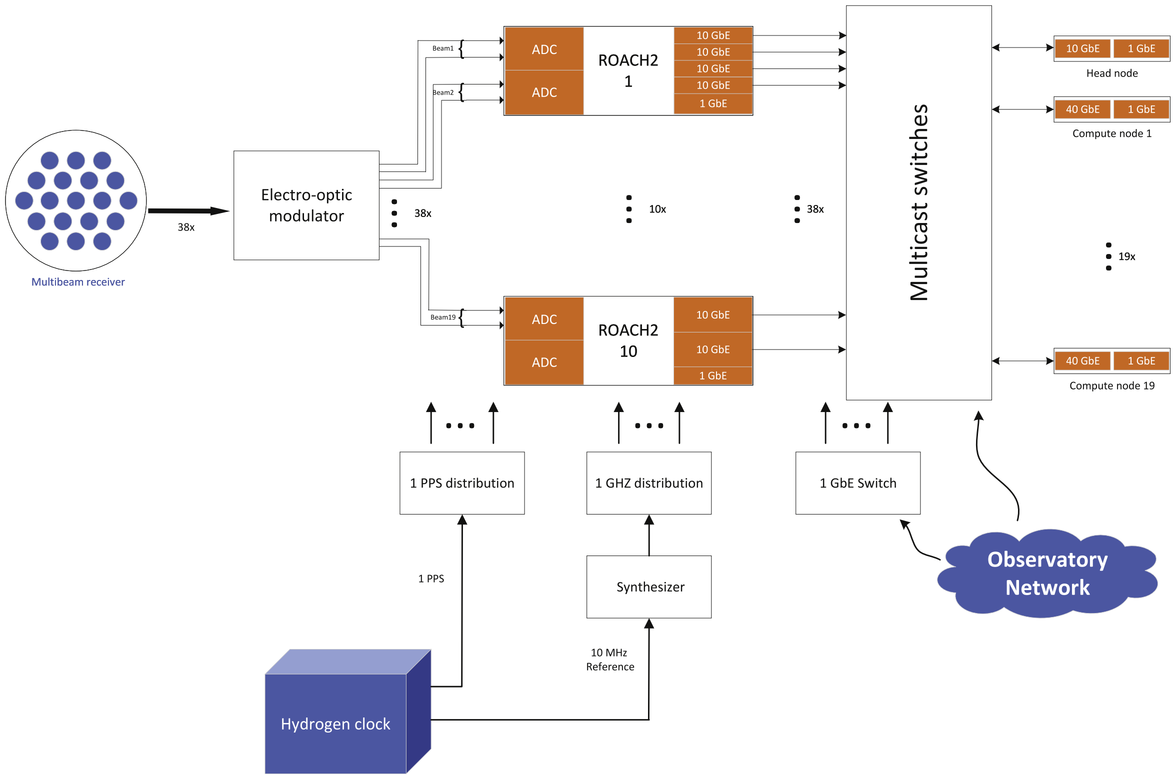

Figure 1. Block diagram of the real-time FRB searching system. This system consists of ten ROACH2 FPGA boxes, one HPC head node and nineteen HPC/GPU compute nodes, connected together with 40 Gb Ethernet switches. The 1 Gb Ethernet is used to monitor and control all ROACH2 boards, and all FRB/SETI head node and compute nodes through the observatory network.

integrated power data into a stream of User Datagram Protocol (UDP) packets, which are then transmitted to each compute node's Ethernet network interface at a data rate of up to 1 GB s^{-1}. The compute nodes primarily perform packet dump and de-dispersion, as well as subsequent calculation work to confirm the candidates, for the FRB real-time searching backend. A head node is responsible for system management, such as adjusting search parameters and validating candidates from each compute node.

3.1. Data Processing Pipeline Diagram

A fundamental issue that the signal processing of the FAST real-time FRB searching backend faces is that as the data rate of the 10 Gb Ethernet network port increases, particularly when it approaches 1 GB s^{-1}, the data receiving system experiences an increasing packet loss rate, while data must still be transferred on time. It is a significant challenge for HPC and software processing performance. We developed three data processing threads and a memory management system based on Hashpipe (MacMahon et al. 2018) for receiving and processing UDP packets, as illustrated in Figure 4. Each procedure is distinct in its functionality. First, the network thread is responsible for receiving and extracting UDP packets and storing them in the assigned input ring buffer. Second, the Cal thread converts the data from two linear to Stokes polarization and writes the values to the output ring buffer. Third, the output thread reads data from the output ring buffer, saves the values in SIGPROC[11] filterbank format, and stores them in the RAM of the compute nodes in preparation for incoherent de-dispersion. Additionally, Hashpipe has developed a corresponding protection mechanism to ensure that the same segment of the ring buffer is not read and written concurrently. Furthermore, this data processing system includes a Hash key interface for monitoring the system's status. Three threads process the data stream in parallel, enabling real-time processing and storage of high-speed data.

3.2. Grouping of 19 Beams

The incoherent de-dispersion search portion of this pipeline is accomplished using Heimdall, a well-developed software application that is employed in the FRB search survey (Barsdell et al. 2012). Each GTX 1080Ti compute node runs the GPU-accelerated software Heimdall. There are options for adjusting the DM search range and boxcar pulse width match. In real-

[11] http://sigproc.sourceforge.net/

Figure 2. The ROACH boards and the HPCs in the Computer Room at the FAST Site.

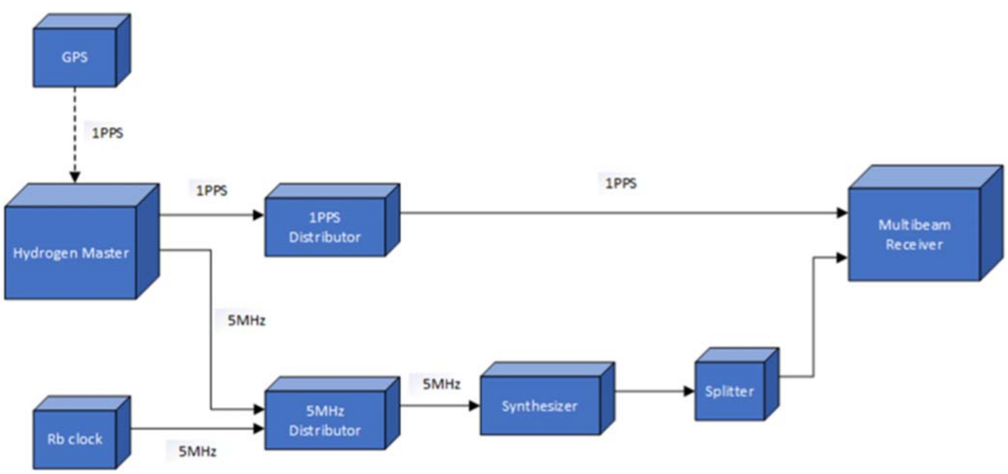

Figure 3. A block diagram of the PPS and clock. The hydrogen master serves as the primary source of high stability for the multi-beam receiver, providing stable 5 MHz and 10 MHz sinusoid signals to the synthesizer's reference input to generate stable clock signals for the ROACH2 onboard ADCs. A secondary frequency standard, which is prepared for emergency situations, is an SRS725 Rb Clock.

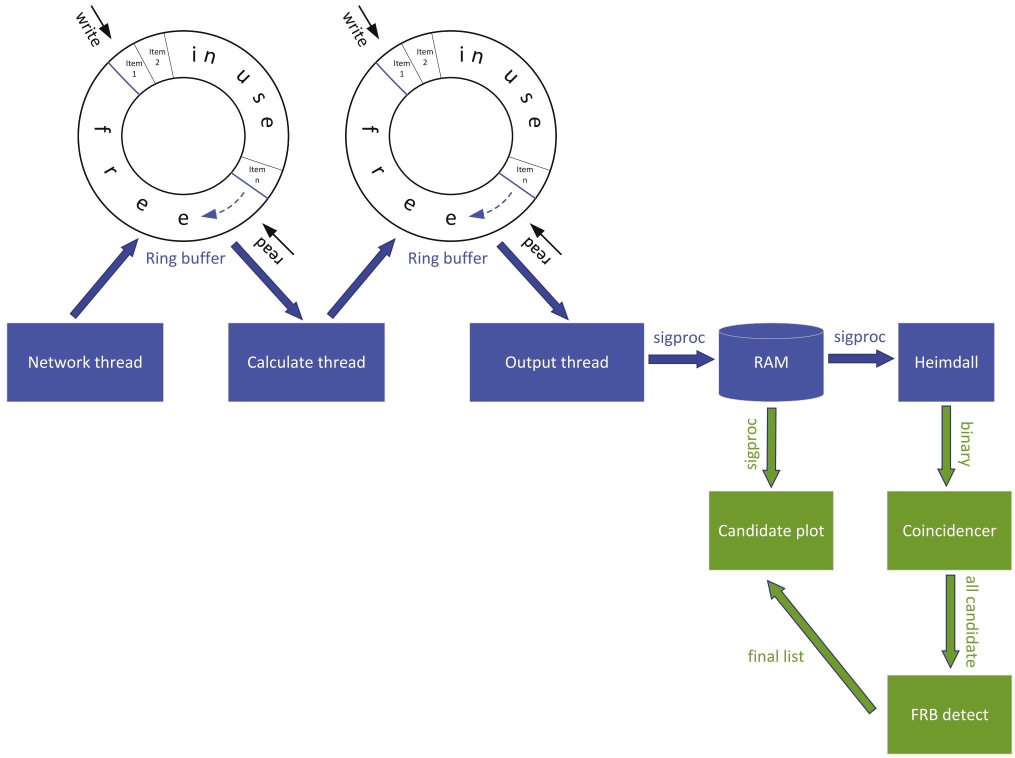

Figure 4. Data processing pipeline diagram. The blue module represents the data processing and calculation on each compute node, while the green module corresponds to the data processing and calculation on the head node. These three threads share the input and output ring buffers, and each ring buffer opens multiple segments to allow for simultaneous writing and reading of data.

time search, the DM range is 20–10,000 pc cm^{-3} with DM step efficiency of 25%, which is the maximum anticipated loss in the S/N due to mismatch between the true DM of the candidate and selected DM steps. A coincidencer daemon is always running on the headnode and is waiting for the said number of beams to arrive. Once the Heimdall finishes processing, all the candidates from compute nodes are transferred across the network to the coincidencer; if there are differences in the time required for packets sent from each beam to reach the head node for whatever reason, and the time difference between the arrived list of candidates is less than ten seconds, a script allocates all nineteen packets; if the time difference is greater than ten seconds, an error is reported in the data record.

The coincidencer collates all candidates from all beams at a given time into a single file. It determines the likelihood of a candidate being Radio Frequency Interference (RFI) by checking for candidate coincidence across multiple beams and adds an RFI flag. If five or more candidates come from distinct beams, or if two or more come from non-adjacent beams, they are most likely RFI. The head node will filter the results based on the beam ID, S/N and time of arrival (Vishal et al. 2022). As an FRB source is a sky-localized point source, it is unlikely to appear in all beams. As a result, this filter will keep RFI out of the local environment.

A process running on each compute node will periodically push the contents of its status buffer to the Redis database on the head node. By subscribing to the predefined channels on the Redis database, this process will be constantly informed of changes to their compute node's status buffer. Once it detects changes, the remote Redis client will publish updates to certain fields in the compute node's status buffer to coordinate the recording pipelines of all compute nodes (Figure 5).

3.3. Decision Mechanism

The beam mask is generated to determine in real time whether the signals searched by Heimdall on 19 compute nodes are RFI or candidates. If a similar signal is detected in a beam, we set the flag to 1. Otherwise, the flag is 0, and a series of 19-bit flag bits plus the binary beam mask table's highest two RFI discriminant bits are generated. For instance, if two similar signals are detected in beams 1 and 2, the binary beam mask will be set to 00 0000000000000000011, and the valid mask will be 3; if four similar signals are detected in beams 2, 3, 9 and 10, the binary beam mask will be set to 00 0000000001100000110, and the valid mask will be 774. We employ the final valid mask tables depicted in Figure 6.

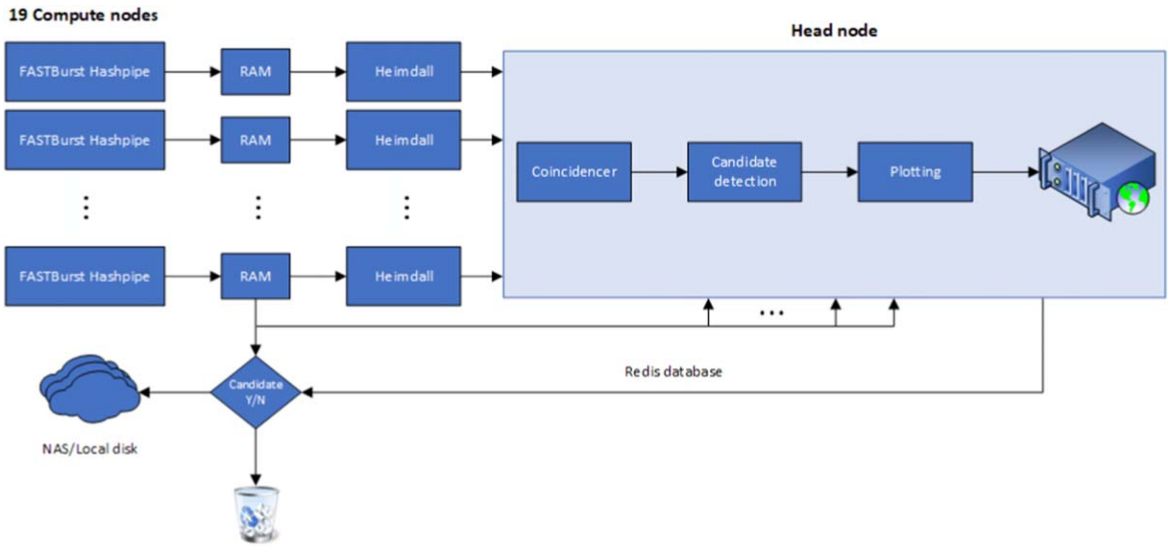

Figure 5. The grouping of the data processing pipeline for the 19 beams. The FASTBurst Hashpipe threads receive the integrated power spectra packets from ROACH2, and reformat and store the data file in RAM temporarily, then the pipeline uses Heimdall to search for dispersed pulses which could be FRB candidates. The light blue area in the right of the diagram represents the final candidate decisions on the head node, once new candidates are found, by checking the RFI flag updated in the Redis database to determine whether to store data files from RAM to disk or delete them.

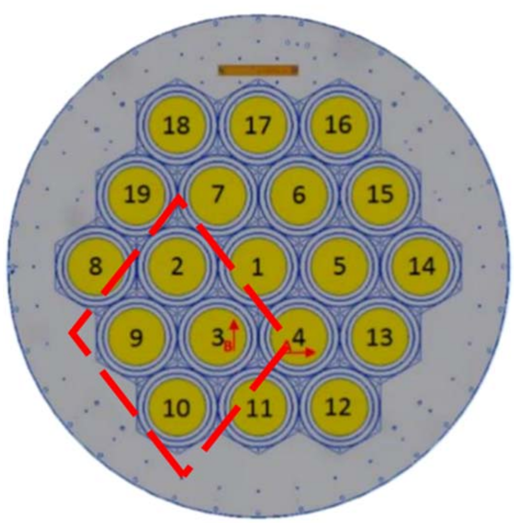

beam number	beam number2	beam number3	beam number4	Binnary beam masks	Valid masks
1	2	3	4	1111	15
1	2	3	7	1000111	71
1	2	3	9	100000111	263
1	2	6	7	1100011	99
1	3	4	5	11101	29
1	3	4	11	10000001101	1037
1	4	5	6	111001	51
1	4	5	13	1000000011001	4121
1	5	6	7	1110001	113
1	5	6	15	100000000110001	16433
1	6	7	17	10000000001100001	65633
1	2	7	19	1000000000001000011	262211
2	3	9	10	1100000110	774
2	3	9	8	110000110	390
2	7	8	19	1000000000011000010	262338
2	7	18	19	1100000000001000010	393282
2	8	9	19	1000000000110000010	262530

Figure 6. RFI discrimination mechanism in the candidate detection. The figure on the left shows the layout of the 19 feeds and the two polarizations, and the table on the other side is the beam combination that might detect the true FRB pulses. We make this binary beam mask table with beam 1, beam 2, from left to right ... all the way to beam 19; once the beam detects a dispersed signal, then the pipeline sets that location to 1 and the remaining locations to 0. Finally, we have a valid mask table which is obtained by converting the binary values to decimal values. The decimal values are used as one of the criteria to determine whether the system detects a real signal.

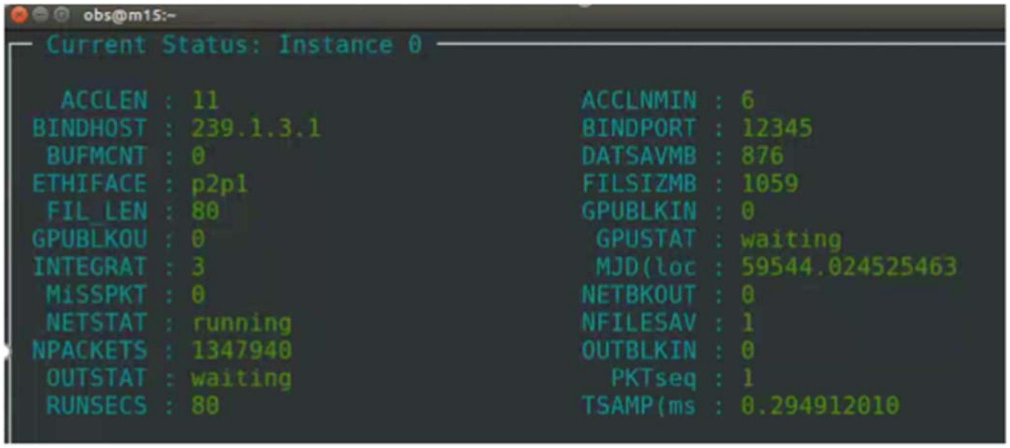

Figure 7. Real-time system monitoring. When a new observation starts, we use this interface to monitor whether the threads of Hashpipe are running properly and to check that the parameters set in the system are correct.

We can adjust the system's minimum detection threshold by adjusting the S/N value, which we have set to 10. Additionally, since the FRB is a point source in the sky, it is unlikely to be detected by more than four beams. Similarly, a large number of FRBs detected at *L*-band are narrower in time so the pulse width threshold, kept close to 128 msec, will not remove any real candidates. Once a new candidate is discovered, this process will also update the state of files in the Redis database with the same start and end times from -1 to 1; otherwise the state of all corresponding filterbank files will remain -1. Each compute node has a demo that constantly reads Redis database entries every ten seconds. When the state of any file changes from -1 to 1, the file is moved from RAM to permanent disk storage. When the state is changed from -1 to 0, those files are deleted from the RAM. Additionally, the system will remove deleted file entries from the Redis database. If a file is not processed for some reason (due to RFI or a header issue) and its state remains unchanged for ten minutes, a cleaner script (daemon running on compute nodes) deletes those files from the RAM to keep it free.

3.4. Plotting and Monitoring

How can we improve the efficiency of the FAST real-time FRB searching system? If the real-time FRB searching system detects an FRB candidate and plots the signal in real-time, the detection efficiency of FRB candidates will be significantly improved. Since all filterbank files in the RAM are mounted on the head node, candidates are extracted and plotted on the head node. A Python script was developed to read output from the detector and then read the Redis database to find out the name of the corresponding filterbank file, then candidates are extracted and plotted on the head node. An example plot from this script is shown in Figure 8. We also use an interface to monitor the running state of each thread, including network port information and real-time input/output ring buffer usage (Figure 7).

4. Commissioning Test

4.1. Onsite Pulse Injection Test

We tested the entire system by injecting a fast birdie into the FAST multibeam receiver twice. Although there was an error in the data collection, we did not see the birdie on the first test, so we repeated the experiment with a stronger birdie.

We used a Rohde & Schwarz SMB100 with a battery inverter that was not locked to the maser, and relied on the internal reference to generate a frequency range from 1400 MHz to 1050 MHz, in 2 MHz steps, with approximately 5 ms per step, a linear, sawtooth and -10 dBm sweep signal into a 1/3 m long wire that emits the birdie on the road near the telescope's edge. Meanwhile, we adjusted the parameters of the real-time FRB searching system to set the integration time to 250 μs, prepare for data reception, and activate the real-time FRB system when we were ready to transmit the birdie. The birdie's signal is depicted in Figure 8.

4.2. Known Pulsar Pointing Test, Example S/N

To confirm the system's capability of searching for single-pulse signals, the high-dispersion pulsar B1900+01 was chosen for trial observation. Then, as demonstrated in Figure 8, we submitted observation plans and successfully detected it; the S/N is approximately 1750.67 and the DM is 244.71.

4.3. Real-time FRB 121102 Burst in 2019 August

At around 00:00(UTC) on 2019 August 30 the FRB terminal was used to conduct routine observations in FAST's main control room when a continuous burst of single pulses with DM between 500 and 600 was discovered. We considered that it was not observed during the previous tracking observation of FRB 121102 and there was no prior

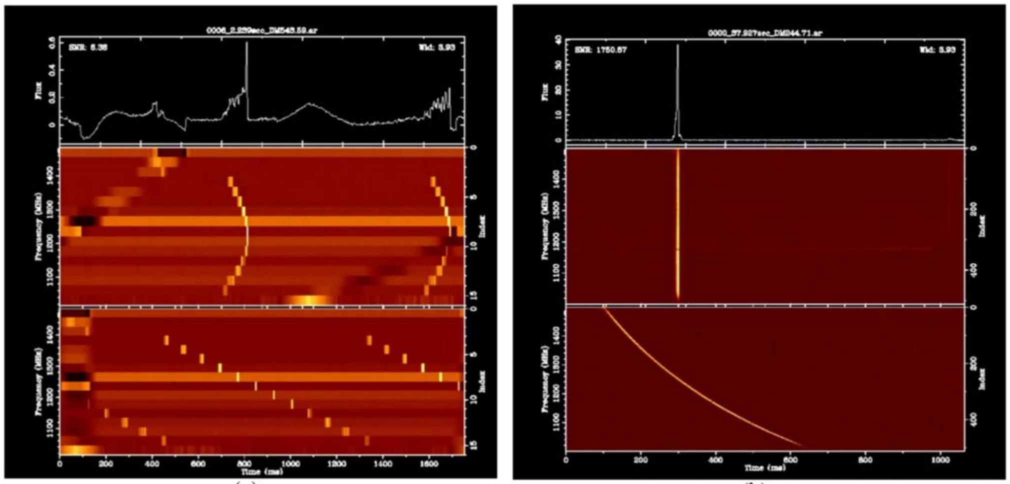

(a) (b)

Figure 8. (a) We successfully found the birdie's signal using the FAST real-time FRB searching system. The top panel illustrates a dedispersed pulse, the middle panel is a dispersed pulse in the frequency–time domain, and the bottom panel shows a dispersed pulse; (b) The successfully identified pulsar B1929+10.

report of an FRB in China. We carefully identified DM and ruled out the possibility of a known RFI. After determining that this could be a genuine burst, we immediately notified the appropriate personnel. The FAST project's debugging team responded immediately, adjusted the observation plan, and scheduled additional time in the early morning for tracking and observing FRB 121102. The signal was still detectable in the follow-up observation, which included one of the bursts captured in real time. We were the first to transmit astronomical telegrams announcing our discovery, alerting our global counterparts to the situation. The Arecibo, Effelsberg and MeerKAT radio telescopes are among the institutions that published their findings. Some of FRB 121102 candidates we detected are displayed in Figure 9.

5. CRAFTS Observation and Event Confirmation

5.1. Day-to-day Observation Strategy

The CRAFTS project is mainly aimed at achieving multiple observations in a limited time (Li et al. 2018). The following is the up-to-date (2021 December 1) CRAFTS sky coverage (superimposed with pulsars) and detailed observation logs, 871.6 hr observed in total, and 130 decl. strips finished starting from 2020 (Figure 10). The FAST real-time FRB searching system is also included in this project, therefore, while observing the spectral lines or searching for pulsars, simultaneously we can search for FRBs.

5.2. Action Determination and Confirmation of Pulsar and FRB

In order to protect the security of FAST network data, the master control servers of the telescope are not connected to the data recording servers, and the real-time location information in the observation cannot be written into files. Therefore, we propose the following two methods to solve the problem that the location cannot be obtained in real time due to the lack of Internet connection. As the first approach (Approach I), we assume that the initial status of the telescope is pointed toward the zenith, and that the initial Modified Julian Date (MJD) and coordinates are recorded. Then, using the burst MJD, the pointing of the central beam can be calculated, as the Earth's motion is easily assumed. For the second approach (Approach II), the FAST control group provided a horizontal coordinate system location function for the feed cabin (X, Y, Z). Rather than using the Earth motion function, we could calculate the feed cabin's relative position. Then, we utilize the Euler rotation matrix, and determine the precise position of the central beam.

Each method has a number of advantages and disadvantages. Approach II is significantly more dependable and precise. However, it must read out the offline information created by the feed cabin file. This constrains the real-time calculation. Approach I can calculate the position in real time, but it would be inaccurate if the telescope had control error, such as the telescope's pointing changing slightly during the observation. Since the location error is typically $< 1'$, Approach I is applied in the real-time FRB searching system.

At the moment, candidates detected by this real-time pipeline are recognized through artificial certification. Once a candidate is found, we will manually enter the information on the candidate into the FAST pulsar database. The system can automatically distinguish the candidate from known pulsars and FRBs. We have also developed a demonstration version of a FAST-Psrcat database access portal (http://47.94.82.12/user/login), which

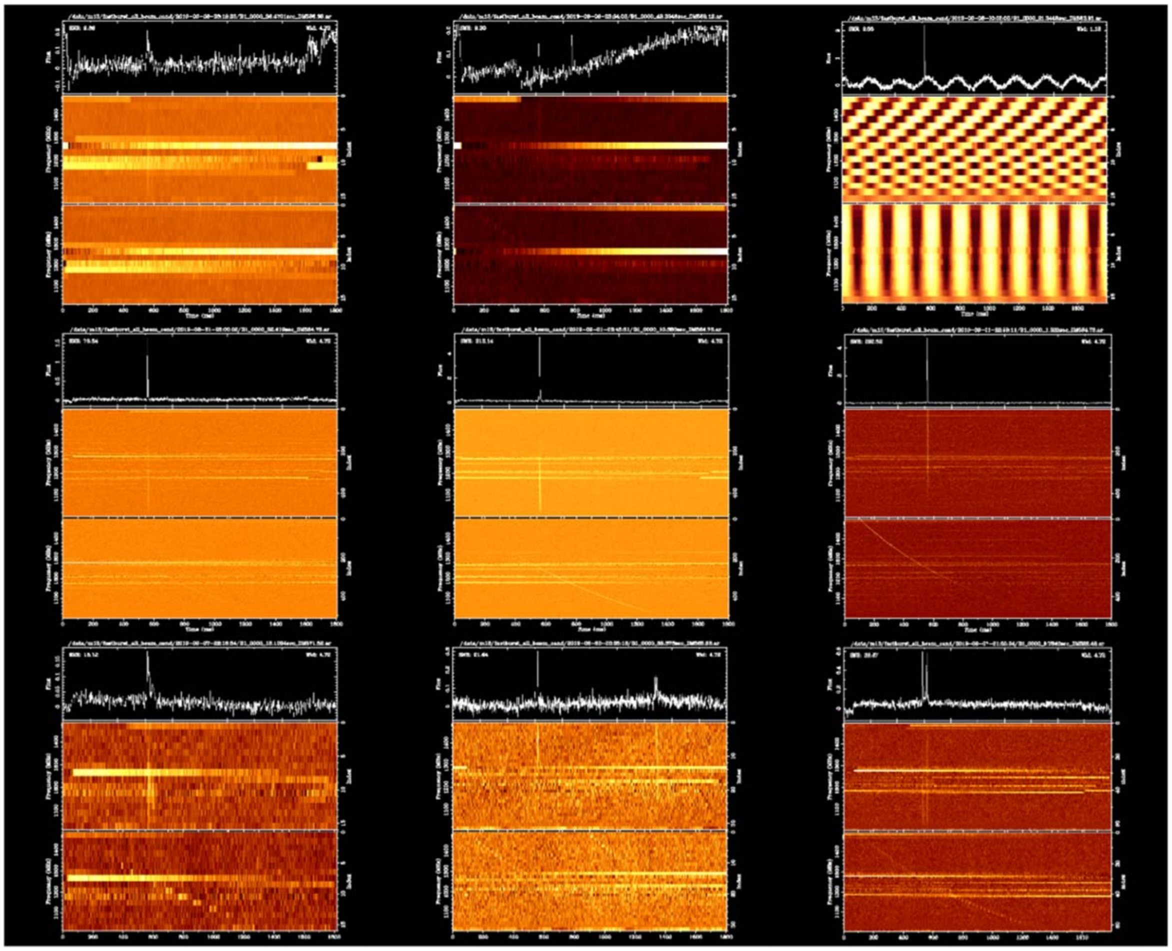

Figure 9. The nine bursts above are some of the more representative FRB 121102 candidates captured by the FAST real-time FRB observations. The top three affirm that candidate signals can still be detected when the signal is weak, with a S/N below 10. The middle three show the observed high S/N candidates. The bottom three feature the observed bimodal candidates. The web server is running and displays the top candidate plots for serendipitous and FRB candidates.

provides a real-time interface to data sets, such as the database of known pulsar ephemerides and records of newly discovered candidates/pulsars from ongoing pulsar surveys (e.g., HTRU, PALFA, CRAFTS). This system enables searching for pulsars based on their rotational parameters, survey identification or regions of the sky, and provides a filter for retrieving a small number of individual catalogs matching the search criteria from the archive. The FAST-Psrcat access portal is currently the only publicly accessible method for identifying pulsar candidates and downloading files. Thus, the user must provide a user name and password to access the portal. In the future, new online public modules based on these data sets will be available.

Using Approach I, we found some pulsars in our observations, and we did some analysis on these detected signals. Due to the high energy of the single pulses, from Figure 11 it can be seen that when utilizing the FAST real-time FRB searching system to detect the signals, some of the pulses are detected from the main and side lobes of the multi-beam. The size of the circles in Figure 12 represents the S/N of the detected signal, and their position from the abscissa axis signifies the distance of the detected signal point from the center origin in this figure. The red line is the average distance from all these points to the origin, and while the 19 beam main lobe is within 3′, it can be seen that most of these signals are detected by the main lobe.

6. Near Future

6.1. Capture of High-precision Spectral Line Data (or Raw Data) Under Event Trigger

The upgraded system will realize the storage of high-precision time-domain raw data based on event triggering, and save the original data for all 19 time-domain beams under trigger.

To obtain the highest-precision spectral line, we will attempt to process the original voltage data directly from the

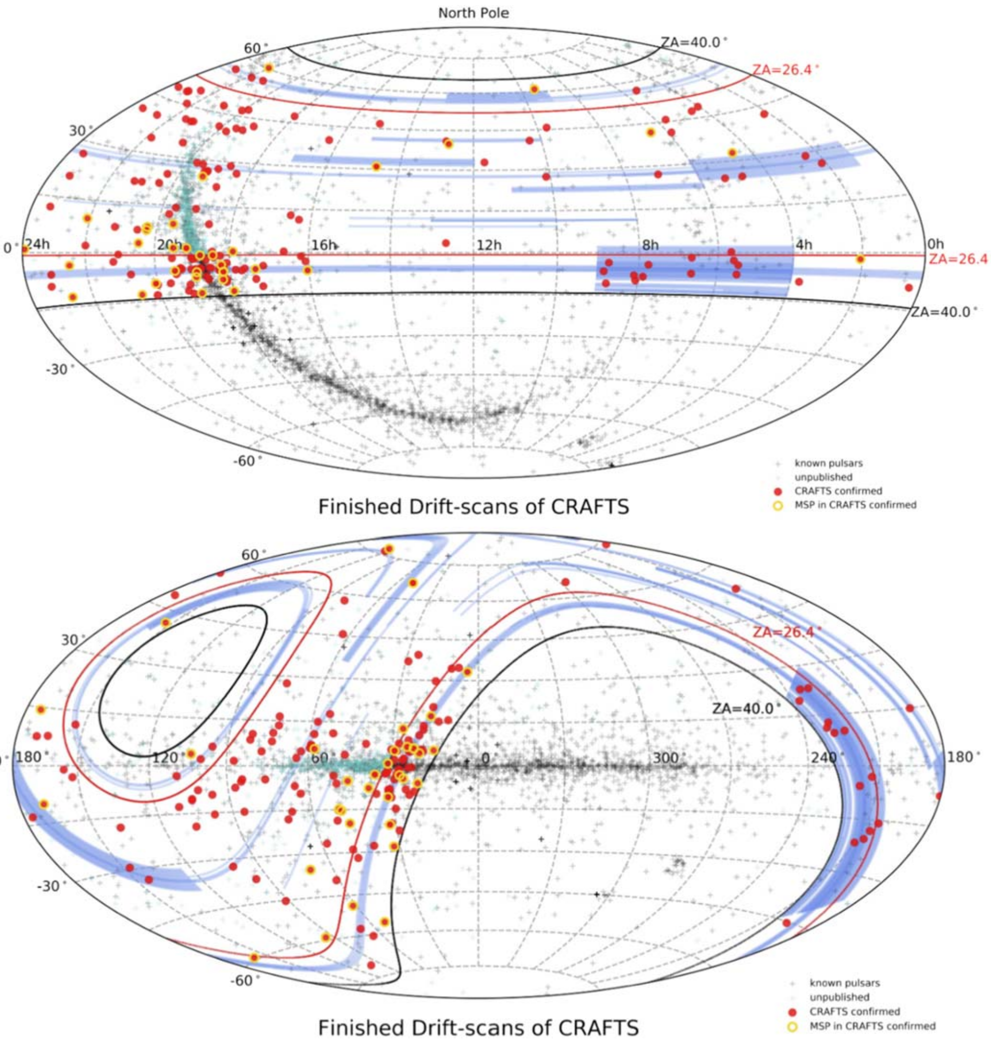

Figure 10. Sky coverage expressed in Equatorial coordinates and sky coverage expressed in Galactic coordinates.

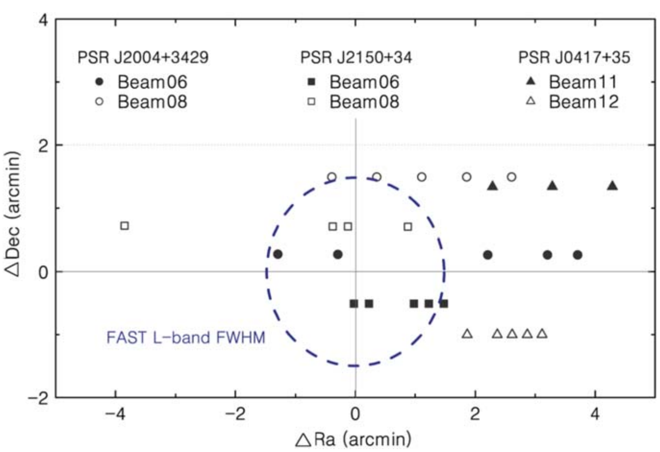

Figure 11. We can either detect the single pulse from the main lobe or the side lobe.

telescope's time domain sampling accuracy. However, this results in unprecedented demands on the overall volume and processing capacity of data. Additionally, storing a large amount of raw data for an extended period of time is implausible. As a result, the system combines the benefits of FPGA and GPU processing, allowing for real-time identification of large amounts of data and establishing an effective trigger mechanism so that the system only stores a few seconds of raw data containing the detected candidate.

6.2. Improving the Ability to Resist Electromagnetic Interference

RFI is a primary concern regardless of whether the observation is of an FRB, a pulsar or a spectral line. This aspect is especially important for FRB observations because the process generates a large number of ineffective candidates,

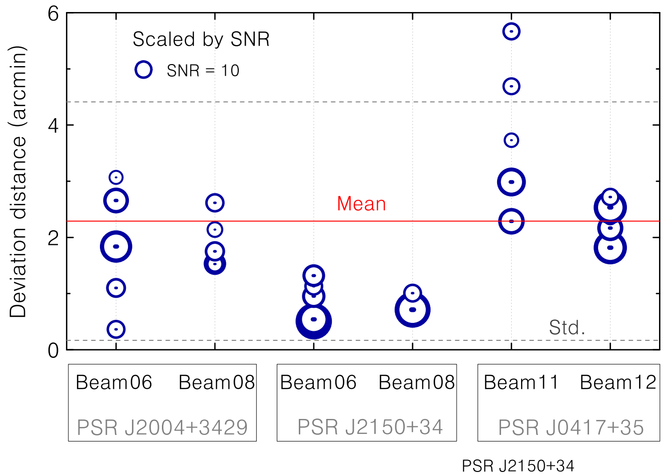

Figure 12. Statistics on pulse detection.

which not only wastes computation and storage time, but also degrades the quality of instantaneous signals such as FRBs.

We consider choosing one of the following two methods to add to our FAST real-time FRB searching system. The first is a fast converging digital adaptive filter, which may be a general solution to deal with RFI with burst and persistent characteristics, broad or narrow band, and tackle fast moving sources or interference with unknown direction of arrival. We have already implemented this system on the ROACH2 platform and tested it at the FAST site, and confirmed that it enables real-time processing of 4096 spectral channels over a 1 GHz bandwidth. The convergence time was approximately 200 μs (Finger et al. 2018), demonstrating the filter's ability to adapt to rapidly changing RFI. The other one is wavelet denoising, which is a technique for rapidly filtering the bandpass and detecting abnormal rises above a predefined threshold. At the same time, it can also be used in conjunction with Principal Component Analysis (PCA) and clustering analysis to identify contaminated channels at wide and narrow bands. After obtaining the list of flagged RFI channels, a statistic about the channel's frequency of occurrence is used to calculate the channel's RFI appearance rate (Yuan et al. 2022). Under the guidance of this rate list, scientists can decide on their own to eliminate channels whose occurrence ratio exceeds a predefined rate for various scientific objects.

6.3. *Optimizing the Head Node's Screening Strategy for Candidates*

We plan to adopt a variant of the coincidence detection algorithm based on spatial filtering techniques (Wang et al. 2022) to optimize the head node's searching strategy for FRB candidates. This technique involves cross correlating pulses in each subband with their lower/higher frequency counterparts, and further using a threshold based on the median average deviation across multiple beams to improve the candidate rankings when processing the data stream in real time. The effectiveness of their method has been confirmed by bright single-pulse detection from known pulsars (Wang et al. 2022). All demonstrated pulsars have been detected separately using the automated pipeline with the FAST *L*-band 19 beam receiver.

6.4. *Improving Parallel Observation Capabilities for Different Observation Modes*

FAST, as the single antenna radio telescope with the highest sensitivity and largest aperture, has a large number of scientific targets and a limited observation time. This has been fully considered in the developed system. By parallelizing with FAST multi-receiver data, and without interfering with FAST's routine observation, the real-time FRB searching system access and operation are enabled. Every day, the observation mode undergoes numerous changes. The FRB backend reading observation plan will be enhanced, onsite electromagnetic interference monitoring data will be read and pulse capture will be automatically coordinated with data from various modes throughout the observation.

7. Conclusion

The FRB searching system developed with the FAST 19 beam receiver has successfully realized multiple detections of FRB 121102, which confirms that FAST can detect FRB signals in real time. While detecting FRBs in real time, we can also record high time resolution data, which can be used for offline processing to study the collected repeated bursts, allowing FRB progenitor models to be scrutinized. Although offline processing has higher time resolution than real-time processing of data, it takes a longer time. Therefore, this is the first time to use the FRB real-time searching system to check whether there are FRBs in the current observation data. If some candidates are detected, then the offline data processing pipeline is utilized to conduct finer research, which makes the observation of FRBs more flexible and efficient. Also for the CRAFTS observations, this real-time searching system also has an automatic process to search for new FRBs. With the upgrade of key technologies in Section 6, the real-time FRB search terminal will further promote the progress of FAST's research on FRBs from discovering phenomena to more thoroughly understanding related mechanisms.

Acknowledgments

This work is supported by the International Partnership Program of the Chinese Academy of Sciences No.114A11-KYSB20200029, the National Natural Science Foundation of China (NSFC, Grant No. 12041301) and the National Key R&D Program of China No.2020YC2201700.

References

Amiri, M., et al. 2019, Natur, 566, 235
Barsdell, B. R., Bailes, M., Barnes, D. G., et al. 2012, MNRAS, 422, 379
Bhandari, S., Keane, E. F., Barr, E. D., et al. 2018, MNRAS, 475, 1427
Chatterjee, S., Law, C. J., Wharton1, R. S., et al. 2017, Natur, 541, 58
Finger, R., Curotto, F., Fuentes, R., et al. 2018, PASP, 130, 025002
Gajjar, V., et al. 2018, ApJ, 863, 2
James, C. W., Prochaska, J. X., Macquart, J. P., et al. 2022, MNRAS, 510, 18
Jiang, P., Yue, Y. L., Gan, H. Q., et al. 2019, SCPMA, 62, 1
Li, D., Wang, P., Qian, L., et al. 2018, IEEE Microwave, 19, 112
Li, D., Wang, P., Zhu, W. W., et al. 2021, Natur, 598, 267
Li, Z. X., Gao, H., Ding, X. H., et al. 2018, NatCo, 9, 1
Lorimer, D. R., Bailes, M., McLaughlin, M. A., et al. 2007, Sci, 318, 777
MacMahon, D. H. E., Price, D. C., Lebofsky, M., et al. 2018, PASP, 2018, 044502
Michilli, D., Seymour, A., Hessels, J. W. T., et al. 2018, Natur, 553, 182
Vishal, G., LeDuc, D., Chen, J., et al. 2022, ApJ, 932, 81
Wang, Y., Zhang, Z., Zhang, H., et al. 2022, A&C, 39, 100568
Yuan, M., Zhu, W. W., Zhang, H. Y., et al. 2022, MNRAS, 513, 4787
Zhang, B. 2018a, ApJL, 854, L21
Zhang, B. 2018b, ApJL, 867, L21
Zhang, X. X., Duan, R., Yu, X. Y., Li, D., et al. 2019, RAA, 20, 073
Zhang, Z. S., Werthimer, D., Zhang, T. J., et al. 2020, ApJ, 891, 174
Zhu, K., Fan, J., Liang, K., et al. 2020, RAA, 20, 072